Thermal Radiation-Driven MHD Nanofluid Flow in a Concentric Cylinder concerning cancer therapy

Mahesha R[1*], Nalinakshi N[2], Sravan Kumar T[3], Sreenivasa T N[4]

1, 2, 3 Department of Mathematics, Atria institute of technology, Bengaluru, KA, India – 560024.
4 Department of Mechanical Engineering, Atria institute of technology, Bengaluru, KA, India – 560024

ABSTRACT:

The aim of current study is to analyze heat transfer in horizontal two concentric cylinders in influence of MHD, internal heat source containing porous nanofluids and thermal radiation are considered. The impact of internal heat source and porous media of H_2O-Cu nanofluids in Lorentz effect are analyzed its applications are cooling system, heat exchangers. Furthermore, using transformation for the momentum and energy equation was applied in this study to obtain a set of ODEs for basic governing equations in the heat transfer flows. In addition, applying a numerical technique of BVP4C method to solve system of non-linear, coupled equations with boundary conditions. The influence of Hartmann number, volume fraction, radiation parameter, internal heat source parameter, Darcy number, and different nanoparticles are examined in velocity and temperature profiles. The results reveal that thermal radiation significantly influence temperature distribution with in the annulus, leading to heat transfer rate. Moreover, the presence of the porous medium and internal heat source modulates the flow patterns. This study provides optimizing MHD nanofluid systems for engineering applications to thermal management system, hyperthermia treatment in cancer therapy, food processing, rotating machinery, and cooling systems. The results are good agreement with the existing work of velocity and temperature graphs.

Key words: MHD, Internal heat source, Porous and Nanofluid medium, Thermal radiation, BVP4C method.

INTRODUCTION:

Heat transfer is the process of transforming heat energy into mechanical energy to improve the efficiency of heat transfer it become a challenging issue in industrial and engineering applications. For the effective heat transfer to analyze in the presence of nanofluids plays a role in cooling/heating effects. Fluid properties such as thermal conductivity, viscosity, stability of nanofluids is high it plays an important role in applications of industry. Firstly, Choi and Eastman [1] investigated nanofluids behaviors in heat transfer analysis. Mixed convection is the convection of both natural and forced investigated by Merkin et al [2]. Natural convection of vertically flat heated plate on external hydromagnetic field in heat and mass transfer is examined by Saini et al [3]. Stability analysis flow of magnetic field investigated numerically by Sangamesh et al [4].

A numerical analysis of free convection MHD over a moving vertical flat plate using Lie group transformation examined by Md. Uddin et al [5]. Heat and mass transfer analysis of free convection in influence of MHD, radiation, and heat generation/absorption over a stretching sheet explained by Salen et al. [6] as result boundary layer thickness increases with increased value of viscosity. Finite element analysis and simulation of steady case over cylinder in the impact of hydromagnetic forces are investigated by [7,8] as result gives magnetic forces

 https://doi.org/10.5281/zenodo.14172363

are opposes the fluid rate, different nanoparticles are analyzed. Heat transfer analysis of unsteady, non-Newtonian, MHD flow in a contracting cylinder and numerical method explained by Saranya and Al-Mdallal [9]. As a result, MHD advances fluid flow rate and $CoFe_2O_4$ nanofluid dominate the fluid flow system. Effect of non-linear electrified jets in electrospinning process is analyzing the bead-spring model investigated by Vahidi et al [10]. The simulations of non-Newtonian rheology observed that elongation dynamics reducing the stable jet length. Besthapu et al. [11] explained thermal radiation, MHD of Casson nanofluid flow over a stretching surface of convective stagnation point it gives Sherwood number demonstrate the significant influenced by Brownian motion and solved Keller's box techniques.

MHD is an electrically conducting fluid in the presence of magnetic field. MHD flow and heat transfer by shrinking permeable sheet of nanofluids are explained by Valipour and Gouran et al [12] as a result an increasing volume fraction temperature profile of skin friction, Nusselt number increases. Saranya and Al-Mdallal [13] investigated numerical analysis of hybrid nanofluids of ferroparticles in a cylinder Legendre Collocation method of unsteady viscous-ohmic dissipative effect are considered. Heat transfer rate and skin friction coefficient is decreases with Eckert number. Comparative analysis of VIM and Runge-Kutta method for accuracy method solved the non-linear vibration of single walled carbon nanotubes by nonlocal Timoshenko beam theory examined by Ghasemi and Ranjbar [14] it shows frequency of single walled carbon nanotubes amplitude increases. Ghasemi and Gouran [15] examined motion of vertically nano droplet in incompressible Newtonian fluids are analysed VIM and HPM techniques as a result the effect of sphericity on velocity, acceleration is analysed. Natural convection of Cu-water based nanofluids between two infinite parallel plates are examined by Dehghani et al [16] it gives thermal boundary layer thickness decreases with increasing volume fraction.

A comparative analysis of MHPM and numerical techniques by rigid rod in a circular surface examined by Ghasemi et al. [17] it shows oscillation amplitude decreases and velocity is maximum at 60^0. Influence of nonlocal parameters high velocity observed in a theoretical analysis of single-walled carbon nanotubes are analysed by Vahidi et al. [18] using Pasternak-type model. Temperature-dependent heat transfer analysis of solid and porous convective fins with different effect such as thermal conductivity, heat generation by DTM method by [19, 20] as a result DTM approach gives more efficiency. Talarposhti et al. [21] investigated analytical Exp-function method to solve Sine-Gordan and Ostrovsky equation of wave equation it gives method is efficiency and plotted contour plots for velocity profiles. Nanofluid flow in two concentric cylinders of KKL model, MHD, thermal radiation effect investigated by Sheikholeslami et al. [22] the result shows temperature enhances the Eckert number and Reynolds number. Sohail et al. [23] investigated heat and mass transfer mathematical analysis of non-linear stretching surface in gyrotactic microorganisms using Brownian and thermophoresis effects it results shows magnetic parameter retard the fluid flow rate. Sohail and Naz [24] examined heat and mass transfer of MHD over a stretching cylinder solved by OHAM and numerical techniques. It gives the results of escalating values of magnetic parameter in velocity profile.

An interesting work is observed in Ghasemi and Hatami [25] analysing solar radiation, MHD with nanofluids over a stretching surface by numerical differential quadrature method it gives more accurate solution and thermal boundary layer thickness increases with Biot number.

 https://doi.org/10.5281/zenodo.14172363

Influence of magnetic field of nanofluid in a hot cylinder is solved by CVFEM method as a result Lorentz force causes fluid flow system is investigated by Sheikholeslami [26, 27] and forced convection Fe_3O_4-Ethylene Glycol based nanofluid heat transfer are analysed. Theoretical analysis of two parallel porous blocks between micropolar fluid are investigated by Valipour et al. [28] and analysed analytically (OHAM), numerically RK method, it gives good results, magnitude of the microrotation velocity high. Gouran et al. [29] examined theoretical analysis of MHD, solar radiation between two concentric cylinders as a result gives Nusselt number enhances the radiation, Hartmann number and analysed DCM and OHAM. Heat transfer analysis of rotating horizontal annulus in the influence of MHD, thermal radiation is examined by Peng et al. [30] and using KKL model RK method solved as a result Hartmann number decreases fluid flow rate. Sushma and kavitha et al. [32, 33] investigated variable fluid properties of mixed convection MHD over a vertical heated plate with porous matrix by numerical method as a result magnetic field diminishes the fluid flow rate.

Based on the above literature survey many authors are ignored to analyse heat transfer between two concentric cylinders in the influence of internal heat generation, MHD, solar radiation, containing nano with porous medium. The impact of MHD, radiation, internal heat generation, nano-porous medium applications are in hyperthermia treatment for cancer therapy, engineering applications such as cooling of nuclear reactors, MHD generators, thermal control system, rotating heat exchangers, solar energy systems, chemical reactors, nanofluidic drug delivery, thermal management in medical devices.

MATHEMATICAL FORMULATION:

Consider steady, laminar, incompressible, unidirectional fluid flow of a two concentric cylinder Cu-H_2O nanofluid are considered. By assuming induced magnetic field is ignored and Lorentz force is applied along fluid flow. Impact of internal heat generation, solar radiation, over two concentric cylinders containing nano with porous medium. Radial axis act upwards and fluid flow along z-axis with T_1 is temperature for r_1, T_2 is temperature for r_2 between two cylinders containing porous nanofluids. In this current problem, the governing equations of Cu-H_2O nanofluids and heat transfer in cylindrical coordinate system with boundary conditions [22, 30] are given by

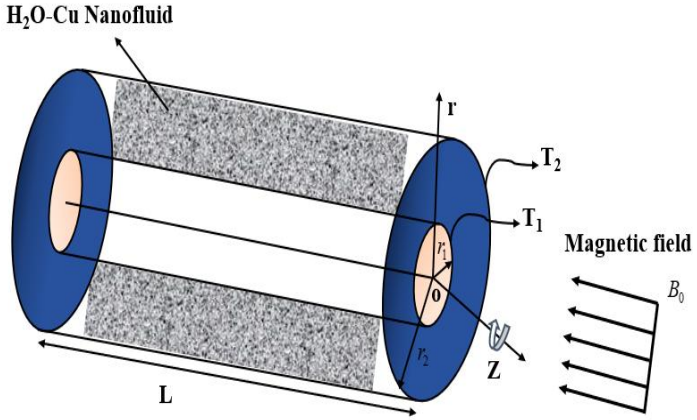

Fig 1. Physical Configuration Flow Problem.

 https://doi.org/10.5281/zenodo.14172363

ISSN: 0369-8963

Conservation of momentum:

$$\upsilon_{nf}\left(\frac{\partial^2 U}{\partial R^2}+\frac{1}{R}\frac{\partial U}{\partial R}-\frac{U}{R^2}\right)-\frac{\sigma_{nf}UB_0^2}{\rho_{nf}}-\frac{U\mu_{nf}}{k\rho_{nf}}=U\frac{\partial U}{\partial R} \tag{1}$$

Conservation of energy:

$$\frac{\kappa_{nf}}{R}\frac{\partial}{\partial R}\left(R\frac{\partial T}{\partial R}\right)+\mu_{nf}\left(\frac{\partial U}{\partial R}-\frac{U}{R}\right)^2-\frac{\partial q_r}{\partial R}-Q_0\left(T-T_2\right)=\left(\rho C_p\right)_{nf}U\frac{\partial T}{\partial R} \tag{2}$$

with the boundary conditions is imparted

$$R=r_1: U\left(R\right)=\omega r_1,\ T=T_1$$

$$R=r_2: U\left(R\right)=0,\ T=T_2 \tag{3}$$

Using the Taylors series expansion and Rosseland approximation heat flux rate of radiation is given by

$$T^4\cong 4T_2^3T-3T_2^4,\ q_r=-\frac{4\sigma_e}{3\beta_R}\frac{\partial T^4}{\partial R} \tag{4}$$

The similarity transformation of above governing equations [22, 30] are

$$r=\frac{R}{r_2},\ u=\frac{U}{\omega r_1},\ \eta=\frac{r_1}{r_2},\ \theta=\frac{T-T_2}{T_1-T_2} \tag{5}$$

The non-dimensional parameters are

$$\mathrm{Re}=\frac{\rho_f\omega r_1r_2}{\mu_f},\ \mathrm{Pr}=\frac{\mu_f\left(\rho C_p\right)_f}{\rho_f\kappa_f},\ Ec=\frac{\rho_f\left(\omega r_1\right)^2}{\left(\rho C_p\right)_f\Delta T},\ N=\frac{4\sigma_eT_c^3}{\beta_R\kappa_f},\ Ha=B_0d\sqrt{\frac{\sigma_f}{\mu_f}},\ Da=\frac{k}{r_2^2}$$

$$Q=\frac{Q_0r_2^2}{\kappa_f},\ S_1=\frac{\rho_{nf}}{\rho_f},\ S_2=\frac{\mu_{nf}}{\mu_f},\ S_3=\frac{\left(\rho C_p\right)_{nf}}{\left(\rho C_p\right)_f},\ S_4=\frac{\kappa_{nf}}{\kappa_f},\ S_5=\frac{\sigma_{nf}}{\sigma_f},\ \eta=\frac{r_1}{r_2} \tag{6}$$

Apply the similarity transformation eqs (5) to above eqs (1-3) using eqs (4 & 6) and Table 1 to form non-dimensional equation are

$$\frac{\partial^2u}{\partial r^2}+\frac{1}{r}\frac{\partial u}{\partial r}-\left\{\frac{Ha^2}{\left(1-\eta^2\right)}\frac{S_5}{S_2}+\frac{1}{r^2}\right\}u-\frac{u}{Da}-\mathrm{Re}\frac{S_1}{S_2}u\frac{\partial u}{\partial r}=0 \tag{7}$$

$$\frac{\partial^2\theta}{\partial r^2}+\frac{1}{r}\frac{\partial\theta}{\partial r}+Ec\,\mathrm{Pr}\frac{S_2}{S_4}\left\{\frac{\partial u}{\partial r}-\frac{u}{r}\right\}^2+\frac{4}{3}\frac{N}{S_4}\frac{\partial^2\theta}{\partial r^2}-\frac{Q}{S_4}\theta-\mathrm{Pr}\,\mathrm{Re}\frac{S_3}{S_4}u\frac{\partial\theta}{\partial r}=0 \tag{8}$$

Dimensionless boundary conditions imparted

$$r=\eta: u=1,\ \theta=1$$

$$r=1: u=0,\ \theta=0 \tag{9}$$

https://doi.org/10.5281/zenodo.14172363

Non-dimensional Skin friction and Nusselt number is given by

$$C_f = -S_2 \left.\frac{\partial u}{\partial r}\right|_{r=\eta} \quad Nu = -S_4\left(1+\frac{4N}{3S_4}\right)\left.\frac{\partial \theta}{\partial r}\right|_{r=\eta} \tag{10}$$

Table 1: Thermophysical properties of spherical-shaped nanofluids [31].

Properties	**Formulas**
Heat capacitance	$\left(\rho C_p\right)_{nf} = (1-\phi)\left(\rho C_p\right)_f + \phi\left(\rho C_p\right)_s$
Thermal expansion coefficients	$\left(\rho\beta\right)_{nf} = (1-\phi)\left(\rho\beta\right)_f + \phi\left(\rho\beta\right)_s$
Thermal diffusivity	$\alpha_{nf} = \dfrac{\kappa_{nf}}{\left(\rho C_p\right)_{nf}}$
Density variation	$\rho_{nf} = (1-\phi)\rho_f + \phi\rho_s$
Dynamic viscosity	$\mu_{nf} = \dfrac{\mu_f}{(1-\phi)^{2.5}}$
Thermal conductivity	$\kappa_{nf} = \kappa_f\left(\dfrac{2\kappa_f - 2\phi\left(\kappa_f - \kappa_s\right) + \kappa_s}{2\kappa_f + \phi\left(\kappa_f - \kappa_s\right) + \kappa_s}\right)$

Table 2: Numerical values of physical properties of Water and different nanoparticles [31].

Property	**Water**	**Ag**	**Cu**	**CuO**
$\rho\left(kgm^{-3}\right)$	997.1	10500	8933	6320
$\mu\left(Pa\,s\right)$	0.00089	-	-	-
$\kappa\left(W\,m^{-1}K^{-1}\right)$	0.613	429	401	76.5
$\beta\times10^{-5}\left(K^{-1}\right)$	21	1.89	1.67	1.80
$C_p\left(J\,kg^{-1}\,K^{-1}\right)$	4179	235	305	531.8
$\sigma\left(\omega m\right)^{-1}$	5.5×10^{-6}	6.3×10^{-7}	5.8×10^{-7}	1×10^{-6}

METHODOLOGY:

The dimensionless flow problem is non-linear and coupled equations with boundary conditions of equations (7-9) are solved numerically by BVP4C method using MATLAB software. By employing this method, to form the set of 1st order ODE's such a $y_1 = r,\ y_2 = u,\ y_3 = \dfrac{\partial u}{\partial r},\ y_4 = \theta,\ y_5 = \dfrac{\partial \theta}{\partial r}$. With the algorithm and corresponding to boundary conditions are

 https://doi.org/10.5281/zenodo.14172363

$$\begin{pmatrix} y_1' \\ y_2' \\ y_3' \\ y_4' \\ y_5' \end{pmatrix} = \begin{pmatrix} 1 \\ y_3 \\ \dfrac{-y_3}{y_1} + \dfrac{y_2}{y_1} + \dfrac{Ha^2}{\left(1-\eta^2\right)} \dfrac{S_5}{S_2} y_2 + \dfrac{y_2}{Da} + \dfrac{\mathrm{Re}\, S_1}{S_2} y_2 y_3 \\ y_4 \\ \dfrac{1}{\left(1+\dfrac{4}{3}\dfrac{N}{S_4}\right)} \left(\dfrac{-y_5}{y_1} - \dfrac{Ec\,\mathrm{Pr}\, S_2}{S_4} \left(y_3 - \dfrac{y_2}{y_1} \right)^2 + \dfrac{Q\, y_4}{S_4} + \dfrac{\mathrm{Pr}\,\mathrm{Re}\, S_3 y_2 y_5}{S_4} \right) \end{pmatrix} \tag{11}$$

and related boundary conditions is $\begin{pmatrix} y_1 \\ y_2 \\ y_3 \\ y_4 \\ y_5 \end{pmatrix} = \begin{pmatrix} \eta \\ 1 \\ u_1 \\ 1 \\ \theta_1 \end{pmatrix}$.

RESULTS AND DISCUSSIONS:

The non-dimensional equations of (7-10) are solved numerically BVP4C method with set of first order ODEs using MATLAB software, Table 2, dimensionless BC's, plotted the velocity and temperature graphs keeping parameters constants such as $\phi = 0.01, \mathrm{Pr} = 6.8,\ \eta = 0.5,\ \mathrm{Re} = 1,\ Ec = 0.01,\ R = 0.1,\ Da = 1,\ Q = 1, Ha = 1$.

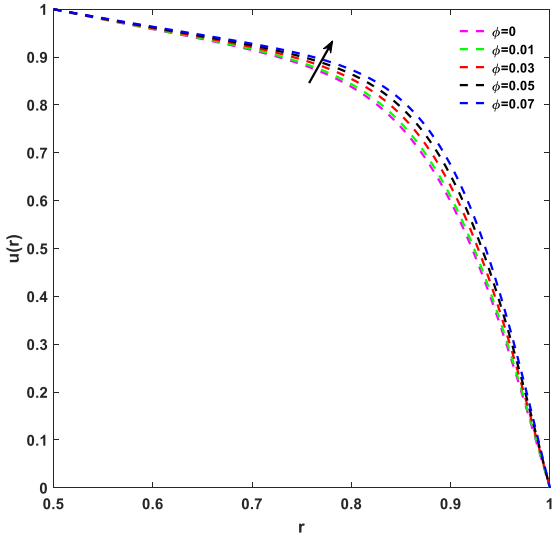

Fig 2. Variation of ϕ on velocity.

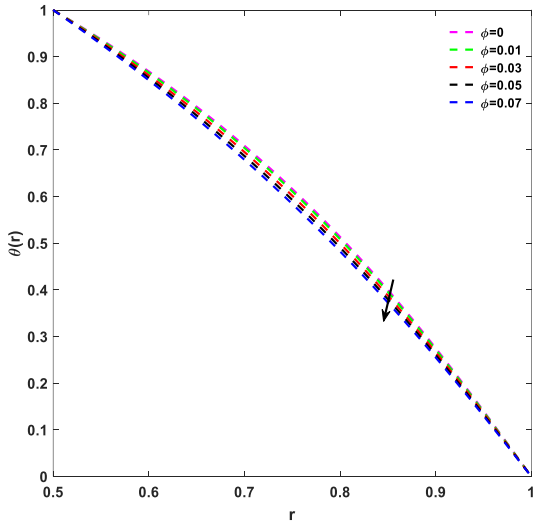

Fig 3. Variation of ϕ on temperature.

https://doi.org/10.5281/zenodo.14172363

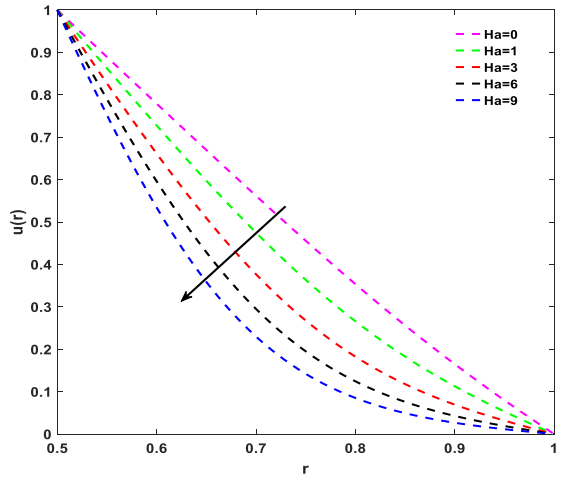

Fig 4. Variation of Ha on velocity.

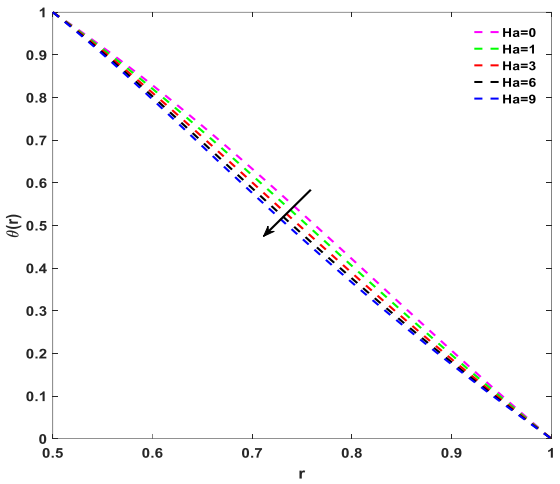

Fig 5. Variation of Ha on temperature.

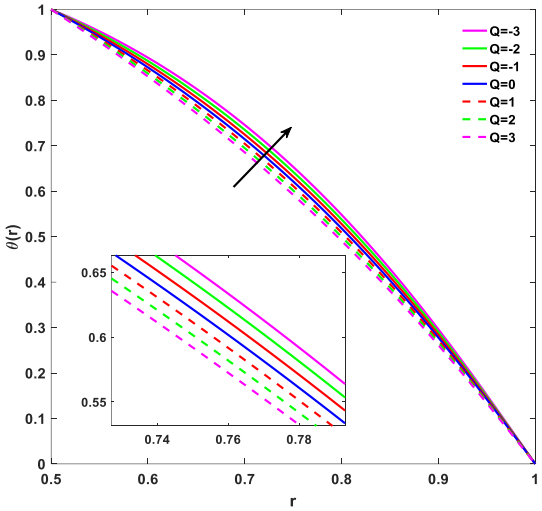

Fig 6. Variation of Q on temperature.

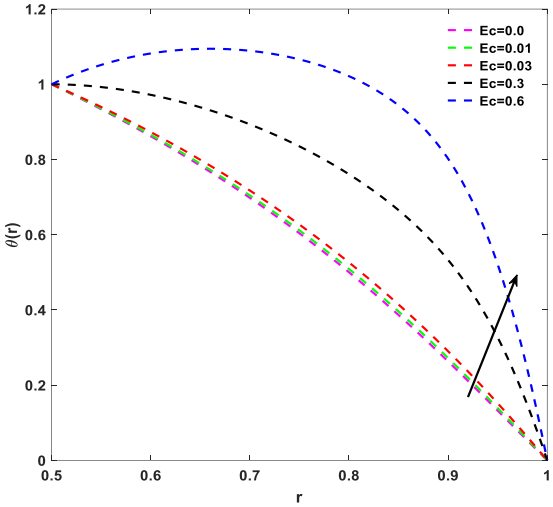

Fig 7. Variation of Ec on temperature.

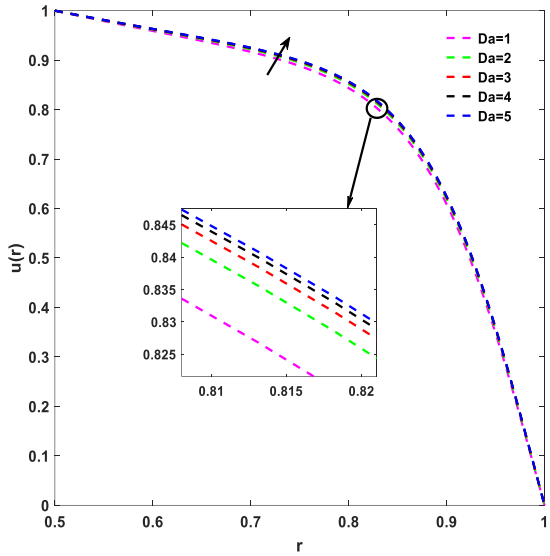

Fig 8. Variation of Da on velocity.

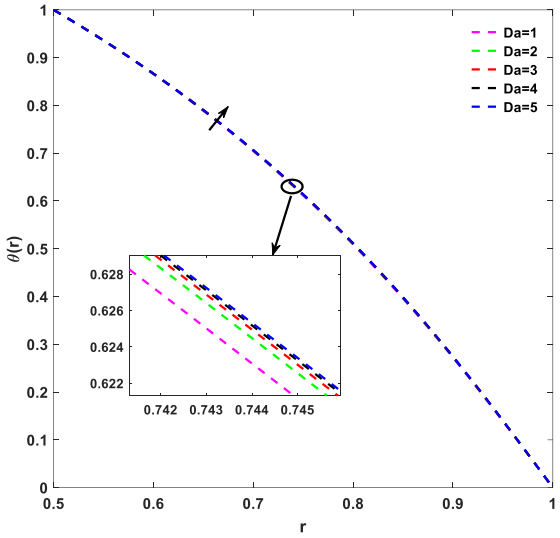

Fig 9. Variation of Da on temperature.

https://doi.org/10.5281/zenodo.14172363

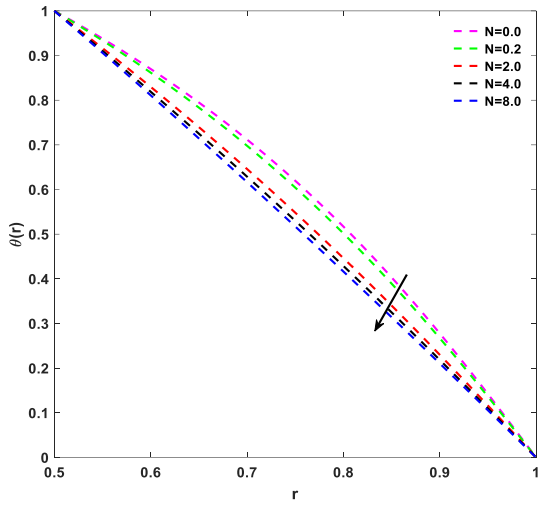

Fig 10. Variation of N on temperature.

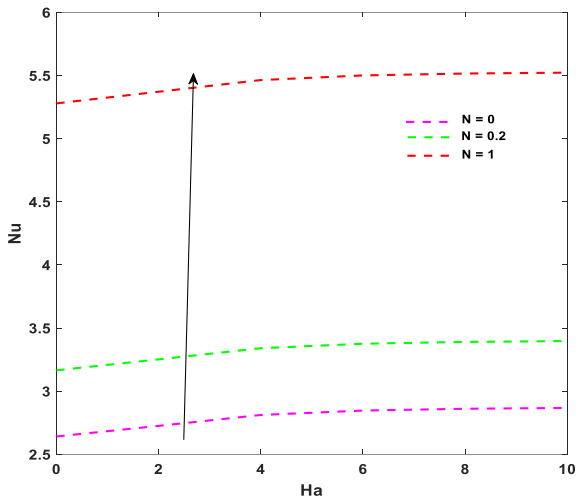

Fig 11. Effect of Nusselt number and Hartmann number on radiation.

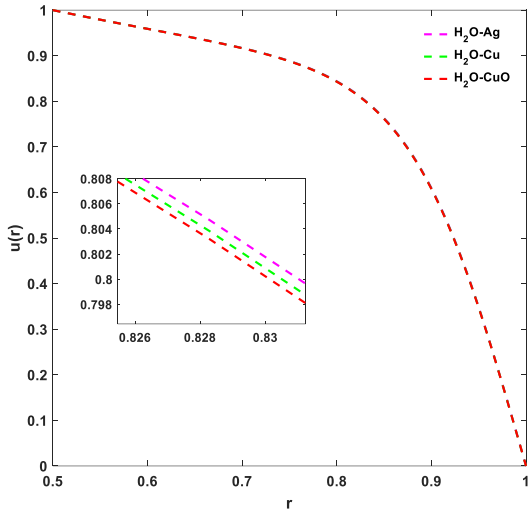

Fig 12. Variation of different nanoparticles on velocity.

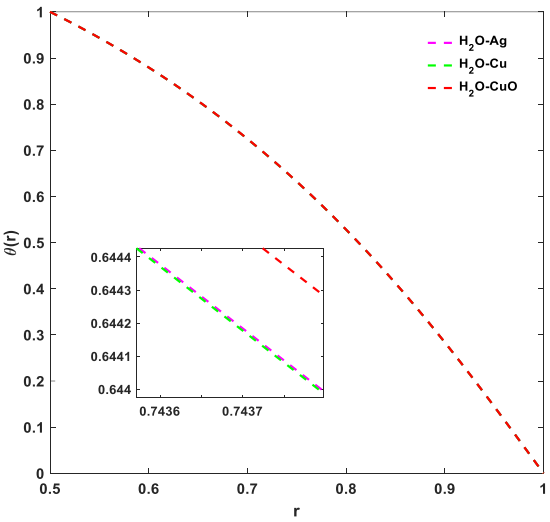

Fig 13. Variation of different nanoparticles on temperature.

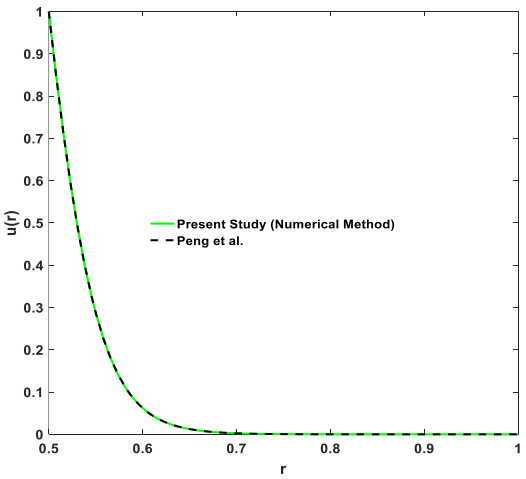

Fig 14. Validation of velocity profile.

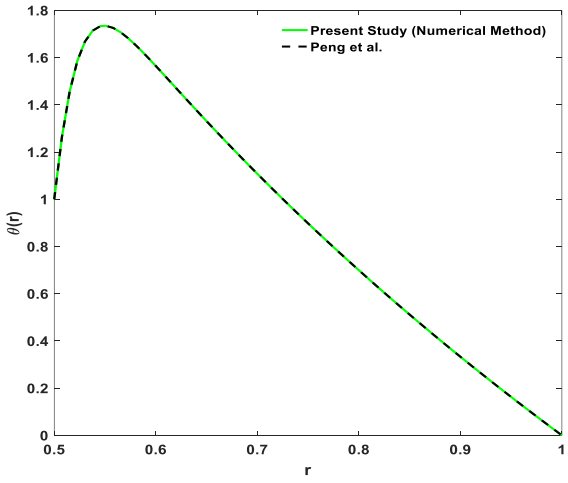

Fig 15. Validation of temperature profile.

https://doi.org/10.5281/zenodo.14172363

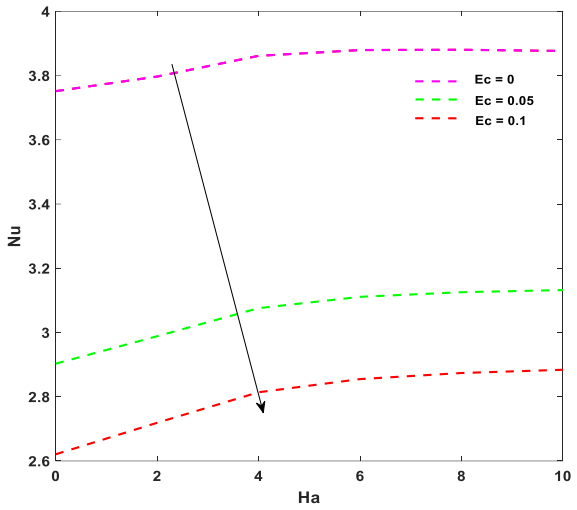

Fig 16. a. Effect of Nusselt number and Hartmann number on Ec.

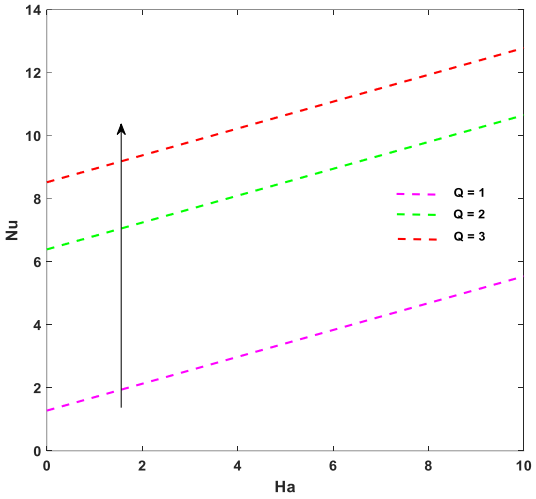

Fig 16. b. Effect of Nusselt number and Hartmann number on Q.

From Fig 2 we observe that an increasing volume fraction velocity increases this is due to increasing density and viscosity it leads to reduction in resistant of fluid flow system and dispersion nanoparticles in fluid causes strong buoyancy force. It is useful in heat exchangers system. In Fig 3 we can analyze volume fraction behaviors in temperature profile. Temperature is decreases as solid volume fraction increases this is because of addition of nanoparticles with higher thermal conductivity leads to overall thermal conductivity of the nanofluid facilitates more efficient heat transfer to its surroundings, heat dispersion is uniform and increased surface area causes reduction in temperature. Its applications in electronic cooling system and automative cooling engine system.

Table 3: validation of the work for velocity and temperature Re=1, Ha=1, Ec=0.1, N=0.2, Da=0.001, Q=0.

r	Velocity - *Peng et al.* [30]	Present study	Temperature - *Peng et al.* [30]	Present study
0.500000000	1.000000000	1.000000000	1.000000000	1.000000000
0.507264546	0.977304817	0.977304814	1.000108603	1.000108605
0.528635994	0.912982911	0.912982920	0.996313234	0.996313236
0.562872313	0.816808808	0.816808809	0.978284458	0.978284459
0.607983813	0.701138961	0.701138963	0.934310258	0.934310260
0.661348778	0.577709577	0.577709579	0.856439761	0.856439763
0.719865830	0.455903028	0.455903030	0.744091562	0.744091566
0.780134170	0.342414779	0.342414781	0.605066162	0.605066167
0.838651222	0.241687777	0.241687780	0.453613121	0.453613124
0.892016187	0.156563181	0.156563184	0.306434992	0.306434995
0.937127687	0.088853094	0.088853096	0.178594509	0.178594510
0.971364006	0.039734716	0.039734717	0.081084505	0.081084507
0.992735454	0.009896650	0.009896651	0.020495729	0.020495730
1.000000000	0.000000000	0.000000000	0.000000000	0.000000000

In Fig 4 & 5 visualize the effect of magnetic force on velocity and temperature plots. An increment in Hartmann number velocity and temperature decreases this is due to Lorentz

https://doi.org/10.5281/zenodo.14172363

force domination by the viscous force and Lorentz force damping effect. Even though convective heat transfer rate drops and suppression of fluid flow leads to reduction in thickness of thermal boundary layer it is useful in MHD pumps and MHD flow control.

Fig 6 shows temperature verses internal heat source parameter. An increasing heat source parameter temperature increases this is because of addition of thermal energy to the system leads to movement of molecules are faster kinetic energy causes temperature gradients increases and applications are circuit analysis in electronic devices. Plotting of viscous dissipation effect by temperature is analyzed in Fig 7 an increasing Eckert number temperature increases due to domination of kinetic energy in fluid flow converts to the thermal energy causes frictional force may lead to viscosity and generation of internal heat rises its useful in hydrodynamic bearings.

Variation of Darcy number are analyzed in Fig 8 & 9 an increasing Darcy number velocity and temperature increases. In the velocity profile understand that applications of efficient filtration process due to presence of porous matrix increased permeability allows large pores fluid flows easily resistance increases it leads to pressure drops. Simultaneously in temperature graph heat transfer is increases because of the increased flow rate and reduced thermal resistance influence of internal heat source its useful in geothermal energy extraction.

Influence of radiation effect on temperature graph observed in Fig 10, as radiation effect increases temperature decreases due to increment in radiation the system radiates more thermal energy leads to a decrease in the overall system internal energy and used in cooling systems. Fig 11 represents the Nusselt number verses Hartmann number for different values of radiation effects, an increasing N values temperature increases at the wall due to friction between fluid and wall of the cylinder. Variation of velocity of different nanoparticles is observed in Fig 12, as H_2O -Ag is high velocity than H_2O-Cu and H_2O -CuO because density and viscosity is higher Ag than Cu and CuO. From Fig 13 observed that temperature is high for H_2O -CuO than H_2O -Ag and H_2O -Cu due to higher thermal conductivity CuO, Ag, Cu. In Fig 14, 15 and Table 3 shows the validation of the velocity and temperature graphs results when $Q = 0, Da = 0.001$ $\phi = 0.01, \Pr = 6.8, Ec = 0.1, N = 0.2, \mathrm{Re} = 1, Ha = 1,$ are in good agreement with existing work of Peng et al. [30].

Effects of Nusselt number (Nu) and Skin friction (C_f) are explained for different parameter plotted in Fig 16. (a & b) Viscous dissipation effect and internal heat source parameter are drawn graphically in Fig 16. (a & b) it shows that an increasing Ec values Nu is decreases and opposite trend observed in Q values Nu is decreases it means intensity are more.

CONCLUSIONS:

This study considered fully developed mixed convection flow of nanofluids, incompressible steady, laminar flow over two concentric cylinders, heat generation, and MHD porous matrix in the presence of solar radiation. The effects of volume fraction, Hartmann number, thermal radiation parameter, internal heat source parameter, Darcy effect, Renolds number are analyzed. The main outcomes of this work are as follows:

1) Influence of thermal radiation reduces the temperature gradient within the annulus, leading to uniform temperature distribution across the flow.

 https://doi.org/10.5281/zenodo.14172363

2) Impact on MHD effects on the nanofluid flow patterns diminish fluid flow rate and stabilizes magnetic field strength.
3) Porous medium acts as resistance to the flow, influenced by thermal radiation and Lorentz force.
4) The combined effects of internal heat generation, thermal radiation, MHD intensifies increased temperature and thermal boundary layer.
5) Intensity of the Nusselt number and Skin friction is more effective with Q, N, η values compare with Re, Ec, values.
6) The study MHD, thermal radiation, internal heat source, porous nanofluids in an annulus is essential for applications in industries such as energy, aerospace, and materials processing, rotating machinery, and heat exchangers.

NOMLECLATURE:

C_p	Specific heat $\left(k\,J/kg.K\right)$		Greek symbols
Ec	Eckert number	ω	Constant rotation velocity
u	Dimensional velocity	α	Thermal diffusivity $\left(m^2/s\right)$
B	Constant applied magnetic field	ϕ	Volume fraction
Pr	Prandtl number	μ	Dynamic viscosity $\left(Pa.s\right)$
Ha	Hartmann number	ρ	Density $\left(kg/m^3\right)$
Nu	Nusselt number	η	Aspect ratio
Re	Renolds number	θ	Dimensionless temperature
N	Radiation parameter		
T	Temperature (K)		
κ	Thermal conductivity of fluid		
Da	Darcy effect		
Q	Internal heat source parameter		

REFERENCES:

1. Choi, S.U.S.; Eastman, J.A.; Enhancing thermal conductivity of fluids with nanoparticles. ASME International Mechanical Engineering Congress and Exposition. **1995.**
2. Merkin, J.H.; Roșca, N.C.; Roșca, A.C.; Pop, I.; MHD Mixed Convection Flow Over a Permeable Vertical Flat Plate Embedded in a Darcy–Forchheimer Porous Medium. Transport in Porous Media, **2024**, 151(13), 2511–2528. https://doi.org/10.1007/s11242-024-02124-6
3. Saini, A.; Negi, A.S.; Kumar, A.; Kumar, A.; Chamkha, A.J.; Radiative convective heat transfer and magneto-hydrodynamic flow in a viscous fluid-saturated porous channel with variable thermal conductivity. International Journal of Ambient Energy, **2024**, 45(1). https://doi.org/10.1080/01430750.2024.2406908
4. Sangamesh; Chamkha, A.J.; K. R. Raghunatha, K.R.; The role of temperature-dependent solubility in the stability of thermohaline convection within a Voigt-fluid layer. Chinese Journal of Physics, **2024**. https://doi.org/10.1016/j.cjph.2024.10.035
5. Md. J. Uddin; Uddin, M.J.; Md. M. Hasan; Faroughi, S.A.; Convective Transport in a Nanofluid-Filled Annulus with an Eccentric Hypocycloid within a Square Disk. **2023**. https://doi.org/10.2139/ssrn.4646931

6. Saleh, M.S.M.; Chamkha, A.J.; Effect of rotating cylinder on nanofluid heat transfer in a bifurcating grooved channel equipped with porous layers. International Journal of Modern Physics B, **2023**, 37, 32. https://doi.org/10.1142/s0217979223502892
7. Rehman, K.U.; Al-Mdallal, Q.M.; Qaiser, A.; Malik, M.Y.; Ahmed, M.N.; Finite element examination of hydrodynamic forces in grooved channel having two partially heated circular cylinders. Case Studies in Thermal Engineering, **2020**, 18, 100600. https://doi.org/10.1016/j.csite.2020.100600
8. Abdelmalek, Z.; Rehman, K.U.; Al-Mdallal, Q.M.; Al-Kouz, W.; Malik, M.Y.; Dynamics of thermally magnetized grooved flow field having uniformly heated circular cylinder: Finite element analysis. Case Studies in Thermal Engineering, **2020**, 21, 100718. https://doi.org/10.1016/j.csite.2020.100718
9. Saranya, S.; Al-Mdallal, Q.M.; Non-Newtonian ferrofluid flow over an unsteady contracting cylinder under the influence of aligned magnetic field. Case Studies in Thermal Engineering, **2020**, 21, 100679. https://doi.org/10.1016/j.csite.2020.100679
10. Vahidi, J.; Akbari, H.; Ghasemi, S.E.; An optimal analytical study on a solar photovoltaic system with different rates of absorbed photon and emitted electron. Results in Engineering, **2023**, 20, 101634. https://doi.org/10.1016/j.rineng.2023.101634
11. Besthapu, p.; Shanker, B.; Alfunsa, P.; Analysis of convective heat transfer in triple diffusive free convection flow of Williamson nanofluid along a horizontal plate. International Journal of Modelling and Simulation, **2023**, 1–10. https://doi.org/10.1080/02286203.2023.2288773
12. Gouran, S.; Vahidi, J.; Akbari, H.; Ghasemi, S.E.; Thermal radiation and porous medium effects on a thin liquid film over a stretching sheet: A numerical comparative study. Case Studies in Thermal Engineering, **2023**, 52, 103753. https://doi.org/10.1016/j.csite.2023.103753
13. Saranya, S.; Al-Mdallal, Q.M.; Javed, S.; Shifted Legendre Collocation Method for the Solution of Unsteady Viscous-Ohmic Dissipative Hybrid Ferrofluid Flow over a Cylinder. Nanomaterials, **2021**, 11(6), 1512. https://doi.org/10.3390/nano11061512
14. Ghasemi, S.E.; Ranjbar, A.A.; Three-dimensional numerical simulation of a laminar fluid flow in an enhanced microchannel with circular protrusions. Mathematical Methods in the Applied Sciences, **2023**, https://doi.org/10.1002/mma.9245
15. Ghasemi, S.E.; Gouran, S.; Mathematical simulation of laminar micropolar fluid flow between two disks for two different geometries. Waves in Random and Complex Media, **2023**, 1–22. https://doi.org/10.1080/17455030.2023.2182139
16. Dehghani, M.R.; Kafi, M.; Nikravesh, H.; Aghel, M.; Mohammadian, E.; Data driven models for predicting pH of CO2 in aqueous solutions: Implications for CO2 sequestration. Results in Engineering, **2024**, 24, 102889. https://doi.org/10.1016/j.rineng.2024.102889
17. Gouran, S.; Vahidi, J.; Akbari, H.; Ghasemi, S.E.; Thermal radiation and porous medium effects on a thin liquid film over a stretching sheet: A numerical comparative study. Case Studies in Thermal Engineering, **2023**, 52, 103753. https://doi.org/10.1016/j.csite.2023.103753
18. Vahidi, J.; Akbari, H.; Ghasemi, S.E.; A new computational approach for velocity components analysis of a solid particle in an incompressible fluid flow. International Journal of Modern Physics C, **2023**, 35, 04. https://doi.org/10.1142/s0129183124500499
19. Ghasemi, S.E.; Valipour, P.; Hatami, M.; Ganji, D.D.; Heat transfer study on solid and porous convective fins with temperature-dependent heat generation using efficient analytical

method. Journal of Central South University, **2014**, 21(12), 4592–4598. https://doi.org/10.1007/s11771-014-2465-7
20. Ghasemi, S.E.; Hatami, M.; Ganji, D.D.; Thermal analysis of convective fin with temperature-dependent thermal conductivity and heat generation. Case Studies in Thermal Engineering, **2014**, 4, 1–8. https://doi.org/10.1016/j.csite.2014.05.002
21. Talarposhti, R.A.; Ghasemi, S.E.; Rahmani, Y.; Ganji, D.D.; Application of Exp-function method to wave solutions of the Sine-Gordon and Ostrovsky equations. Acta Mathematicae Applicatae Sinica, English Series, **2016**, 32(3), 571–578. https://doi.org/10.1007/s10255-016-0571-z
22. Sheikholeslami, M.; Nimafar, M.; Ganji, D.D.; Nanofluid heat transfer between two pipes considering Brownian motion using AGM. Alexandria Engineering Journal, **2017**, 56(2), 277–283. https://doi.org/10.1016/j.aej.2017.01.032
23. Sohail, M.; Naz, R.; Shah, Z.; Kumam, P.; Thounthong, P.; Exploration of temperature dependent thermophysical characteristics of yield exhibiting non-Newtonian fluid flow under gyrotactic microorganisms. AIP Advances, **2019**, 9, 12. https://doi.org/10.1063/1.5118929
24. Sohail, M.; Naz, R.; Modified heat and mass transmission models in the magnetohydrodynamic flow of Sutterby nanofluid in stretching cylinder. Physica A: Statistical Mechanics and its Applications, **2020**, 549, 124088. https://doi.org/10.1016/j.physa.2019.124088
25. Ghasemi, S.E.; Hatami, M.; Solar radiation effects on MHD stagnation point flow and heat transfer of a nanofluid over a stretching sheet. Case Studies in Thermal Engineering, **2021**, 25, 100898. https://doi.org/10.1016/j.csite.2021.100898
26. Sheikholeslami, M.; Magnetic source impact on nanofluid heat transfer using CVFEM. Neural Computing and Applications, **2016**, 30(4), 1055–1064. https://doi.org/10.1007/s00521-016-2740-7
27. Sheikholeslami, M.; Investigation of Coulomb force effects on ethylene glycol based nanofluid laminar flow in a porous enclosure. Applied Mathematics and Mechanics, **2018**, 39(9), 1341–1352. https://doi.org/10.1007/s10483-018-2366-9
28. Valipour, P.; Ghasemi, S.E.; Vatani, M.; Theoretical investigation of micropolar fluid flow between two porous disks. Journal of Central South University, **2015**, 22(7), 2825–2832. https://doi.org/10.1007/s11771-015-2814-1
29. Gouran, S.; Mohsenian, S.; Ghasemi, S.E.; Theoretical analysis on MHD nanofluid flow between two concentric cylinders using efficient computational techniques. Alexandria Engineering Journal, **2022**, 61(4), 3237–3248. https://doi.org/10.1016/j.aej.2021.08.047
30. Peng, Y.; Alsagri, A.S.; Afrand, M.; Moradi, R.; A numerical simulation for magnetohydrodynamic nanofluid flow and heat transfer in rotating horizontal annulus with thermal radiation. RSC Advances, **2019**, 9(39), 22185–22197. https://doi.org/10.1039/c9ra03286j
31. Sravan Kumar, T.; Dinesh, P.A.; Makinde, O.D.; Impact of Lorentz Force and Viscous Dissipation on Unsteady Nanofluid Convection Flow over an Exponentially Moving Vertical Plate. Mathematical Models and Computer Simulations, **2020**, 12(4), 631–646. https://doi.org/10.1134/s2070048220040110
32. Susma, T.C.; Nalinakshi, N.; Dinesh, P.A.; Jayalakshmamma, D.V.; Sravan Kumar, T.; Convective heat transfer and MHD flow through semi-porous cylindrical filters embedded in an impermeable region. Chinese Journal of Physics, **2023**, 81, 9–25. https://doi.org/10.1016/j.cjph.2022.10.015

33. Kavitha, S.; Nalinakshi, N.; Dinesh, P.A.; Brijesh; Analysis of Forchheimer Effect for Double Diffusive Convection With Dusty Fluids and MHD. Journal of Mines, Metals and Fuels, **2023**, 2289–2299. https://doi.org/10.18311/jmmf/2023/36331